

Stability Analysis of Middle Rock Pillar and Cross-Section Optimization for Ultra-Small Spacing Tunnels

Wang Shuren^{1,2,*}, Shi Kunpeng¹, Chen Wenxue^{1,3} and Liu Shiping¹

¹International Joint Research Laboratory of Henan Province for Underground Space Development and Disaster Prevention, Henan Polytechnic University, Jiaozuo 454003, China

²School of Mining Engineering, University of New South Wales, Sydney, NSW 2052, Australia

³Department of Building, Civil & Environmental Engineering, Concordia University, Montreal, QC H3G 1M8, Canada

Received 23 December 2017; Accepted 30 June 2018

Abstract

The ultra-small spacing tunnel is a new tunnel type under the urban engineering environment, which not only has high requirements for deformation and settlement control, but also has great difficulty in construction technology. Since the middle rock pillar is the key part in the design and construction of ultra-small spacing tunnels, to explore the stability of the middle rock pillar in the ultra-small spacing (0-200 mm) subway tunnels, this study examined the Gangding-Shipaiqiao ultra-small spacing tunnels on Guangzhou Metro Line 3 in China by using ABAQUS and theoretical analysis, which mainly involved the plastic zone of the surrounding rock, the stress distribution and skew displacement effect of the middle rock pillar by defining the skew coefficient. The tunnel cross-sections of three different types were optimized, and a simplified calculation method was proposed with the load and ultimate bearing capacity of the middle rock pillar. Results show that the theoretical analysis of the bearing capacity of the middle rock pillar is essentially consistent with the results of numerical calculation. The conclusions obtained in the study are of important theoretical value to provide on-site engineering construction guidance.

Keywords: Double-track tunnel, Ultra-small spacing, Cross-section, Middle rock pillar

1. Introduction

China Metro Design Code stipulates that the net distance between two parallel tunnels should not be less than the diameter of the tunnel outline. In the design stage, the small spacing tunnels scheme should be avoided as far as possible. However, due to the existing building foundation, existing structures, existing tunnels and other conditions around the subway line, it is sometimes unavoidable to use a ultra-small spacing tunneling scheme [1].

With the development of urban construction and the increase of subway lines, small spacing and ultra-small spacing tunnels continue to emerge. The problem of displacement skew effect and surface subsidence caused by the small rock pillars in the construction of ultra-small spacing tunnels are not covered by the current construction specifications in China, and there is no mature construction method reference. Therefore, the stability and control technology of the middle rock pillar in the ultra-small spacing tunnels becomes an urgent technical problem.

In this study, taking the shallow buried ultra-small spacing tunnels between Gangding Station and Shipaiqiao Station (Gangshi sector) on line 3 of the Guangzhou subway as on-site engineering background, we established the numerical model and theoretical model to investigate the stability and control technology of the middle rock pillar in the ultra-small spacing tunnels.

2. State of the art

Currently, plenty of scholars have studied the interaction between the two small spacing tunnels and have evaluated the safety and the minimum width of the rock pillar using numerical analysis methods [2-3]. Mortazavi et al. discussed the failure mechanism and studied the influence of geometry and strength parameters on the performance of rock pillar [4]. Chen et al. analyzed the width effects of rock pillars in multi-line parallel tunnels and found that the interactions became increasingly obvious with the rock pillar width decrease [5]. Zhang and Goh studied the peak vertical stress in the rock pillar and identified the overlap plastic zones [6]. Other scholars have analyzed the deformation characteristics and stress distribution of the middle rock pillar under different construction conditions [7-11]. All the above mentioned studies involved the small spacing tunnels, but the ultra-small spacing (0-200 mm) subway tunnels and the skew displacement effect of the middle rock pillar have been less reported.

For the cross-section optimization of the small spacing tunnels, Wang et al. analyzed the large-span twin tunnels and proposed an optimum flat ratio based on the engineering conditions [12-13]. Han et al. analyzed the deformation of the surrounding rock and the support for the horseshoe section tunnel, and they concluded that a circular section could effectively control both the deformation and the deformation rate of the surrounding rock [14]. However, these authors only optimized one horseshoe section or one circular section for a single-line tunnel, to optimize different

*E-mail address: w_sr88@163.com

ISSN: 1791-2377 © 2018 Eastern Macedonia and Thrace Institute of Technology. All rights reserved.

doi:10.25103/jestr.113.20

3.2.1 Building the computational model

As shown in Figure 2, the cross-section of the double-track tunnel with a clear distance about 190 mm was selected, and the computational model was built by using ABAQUS technique. To reduce the boundary effect, the left-hand, right-hand and lower boundaries of the model were three to four times the excavation diameter of the tunnel. The left-hand and right-hand boundaries of the model were constrained by the lateral displacements, the bottom boundary was constrained by the vertical displacement, and the upper boundary was free. It was assumed that the surrounding rock of the tunnels conformed to the Mohr-Coulomb yield criterion.

As seen from Table 1, the surrounding rock of the tunnels mainly related to grades III, IV and V, and its physical and mechanical parameters were selected according to the China Code for the Design of Highway Tunnels and the China Guide to the New Austrian Method for Railway Tunnels.

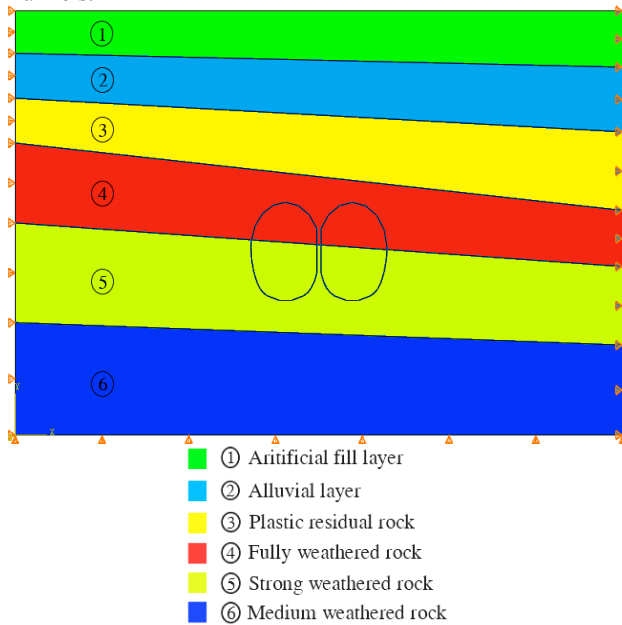


Fig. 2. The computational model and its boundary conditions

Table. 1. Calculating parameters for the model

Grade	Density (kN/m ³)	Elastic modulus (GPa)	Poisson's ratio	Frictional angle (°)	Cohesion (MPa)
III	26	7.0	0.26	39	1.40
IV	23	2.2	0.33	30	0.20
V	20	0.6	0.38	25	0.08

3.2.2 Simulating excavation sequences

The benching excavation method from top to bottom was used for the two tunnels excavation. The left-hand tunnel was excavated first and then the right-hand tunnel. This simulation process could be divided into five main steps: (i) setting the boundary conditions and initial stress balance, then setting the displacement field and velocity filed be zero. (ii) carrying out excavation and support for the upper part of the left-hand tunnel. (iii) carrying out excavation and support for the lower part of the left-hand tunnel. (iv) carrying out excavation and support for the upper part of the right-hand tunnel. (v) carrying out excavation and support for the lower part of the right-hand tunnel.

As shown in Figure 3, the monitoring points of displacement and stress were installed at three key locations of the middle rock pillar to observe the deformation and mechanical characteristics of these positions.

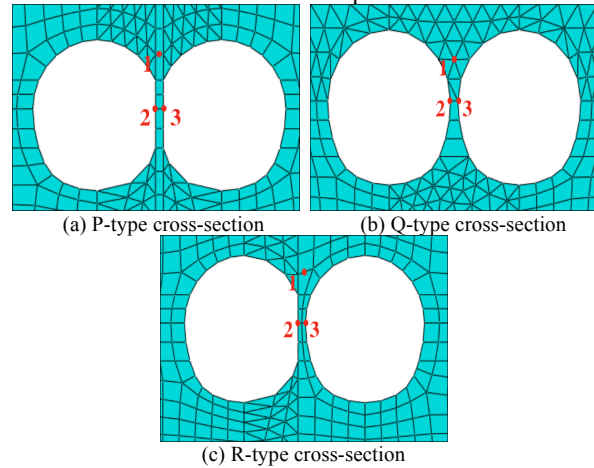


Fig. 3. Monitoring points layout for three different cross-sections

3.3 Ultimate and actual loads theoretical analysis

3.3.1 Actual load calculation of the middle rock pillar

Some assumptions of theoretical analysis[15]: (i) for the shallow buried tunnels, the overburden is homogeneous and it can be considered to be a uniform vertical load. (ii) Since the horizontal stress is smaller than the vertical stress, so only the vertical stress can be considered in the calculation. (iii) The cross-section shape of the two tunnels is selected P-type as showed in Figure 3(a). (iv) it can be assumed that the shear stress in the centre axis of the rock pillar is zero.

Based on the above mentioned assumptions, the bearing range of the middle rock pillar of the ultra-small spacing tunnels can be determined as shown in Figure 4

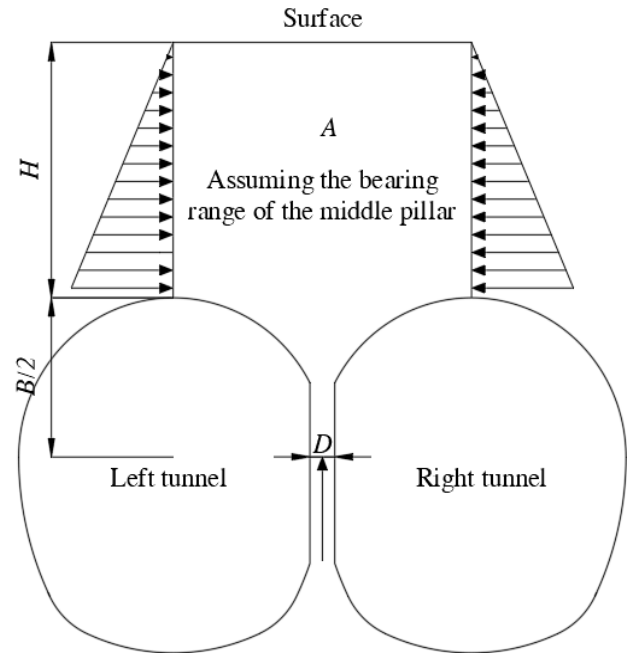


Fig. 4. Bearing range for the rock pillar in P-type cross-section tunnels The vertical stress σ_p of the middle rock pillar can be obtained from the vertical forces balance:

$$\sigma_p \times D = \gamma \times A \tag{1}$$

where A is the bearing area of the middle rock pillar, D is the width of the middle rock pillar, and γ is the weight of the overburden over the tunnels.

The bearing area A of the middle rock pillar can be obtained from the geometric relationship:

$$A = \frac{4-\pi}{8} B^2 + \left(\frac{B}{2} + H\right) D + HB \quad (2)$$

where H is the depth of the tunnels, and B is the span of the two tunnels.

According to the above equations, the formula for the vertical stress σ_p in the middle rock pillar can be obtained:

$$\sigma_p = \frac{\gamma \times B}{D} \left(\frac{4-\pi}{8} + H\right) + \gamma \left(\frac{B}{2} + H\right) \quad (3)$$

3.3.2 Ultimate load calculation of the middle rock pillar

In 1972, Wilson put forward the theory of progressive failure[16]. Through the repeated loading experiments on rock pillars, an equation for the ultimate strength σ_1 of the rock column was obtained as follows:

$$\sigma_1 = \frac{2c \cos \phi}{1 - \sin \phi} + \frac{1 + \sin \phi}{1 - \sin \phi} \gamma H \quad (4)$$

where ϕ is the internal friction angle of the overburden, c is the cohesion of the overburden, γ is the weight of the overburden, and H is the mining depth.

Since the height L of the rock pillar is far larger than its width a , a strip rock pillar can be regarded as a plane problem, and the edge effects at the front and rear of the strip rock column can therefore be ignored. The ultimate load σ_s on a strip rock pillar is as follows:

$$\sigma_s = \left(\frac{2c \cos \phi}{1 - \sin \phi} + \frac{1 + \sin \phi}{1 - \sin \phi} \gamma H\right) (a - Y) L \quad (5)$$

where L is the height of the rock pillar, a is the width of the rock pillar, and Y is the length of the yield zone.

4. Results and discussion

4.1 Failure characteristics of the middle rock pillar

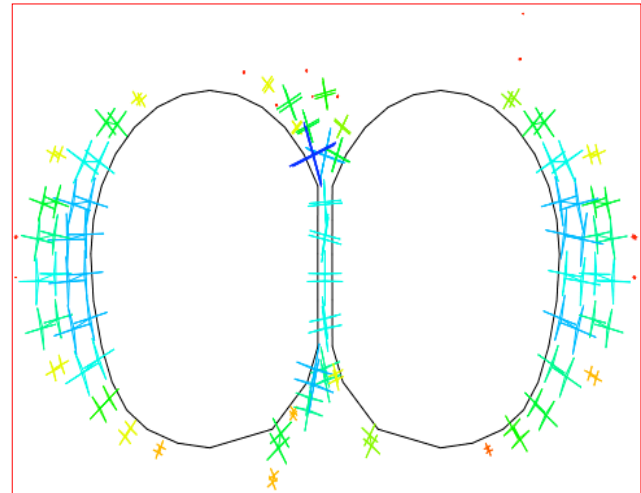
As seen from Figure 5, the plastic failure zones in the surrounding rock of grade V are roughly symmetrical along the middle rock pillars of the two tunnels. The plastic failure zones of the surrounding rock start from the arched waists of the left- and right-hand tunnels, and its range gradually expands toward the surface. In addition, the centralized areas of the plastic zones in the middle rock pillar are more obviously, so the effective supporting measures must be taken to ensure the stability of the rock pillar.

For the plastic failure zones in three cross-sections tunnels, Q-type cross-section is the best, R-type cross-section is the worst, and P-type cross-section is in the middle.

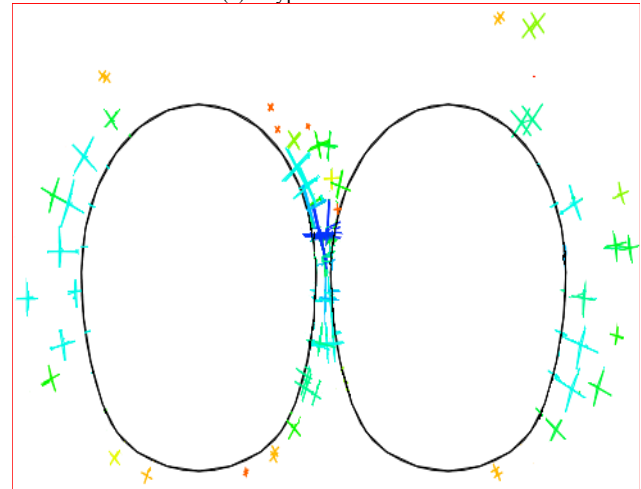
4.2 Vertical stress analysis of the middle rock pillar

Due to the excavation of the shallow buried ultra-small spacing tunnels, the smallest distance between the two tunnels is the waist of the middle rock pillar, which is the weakest place and the most likely to cause damage.

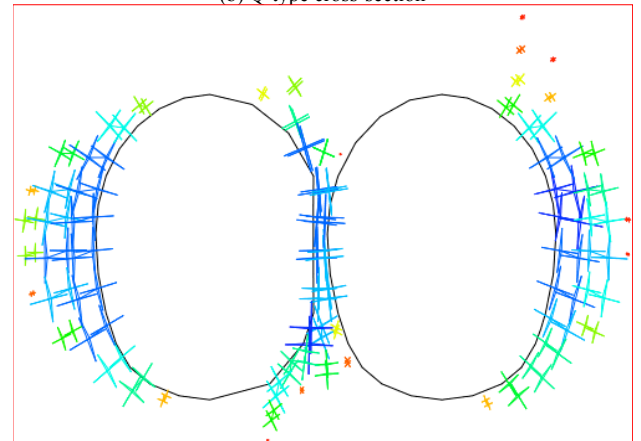
As seen from Figure 6, it can be seen that the maximum vertical stress occurs at the waist of the middle rock pillar. For the maximum compression stress in three cross-section tunnels, Q-type cross-section is the smallest 7.80 MPa, R-type cross-section is the biggest 9.17 MPa, and P-type cross-section is in the middle 8.63 MPa.



(a) P-type cross-section

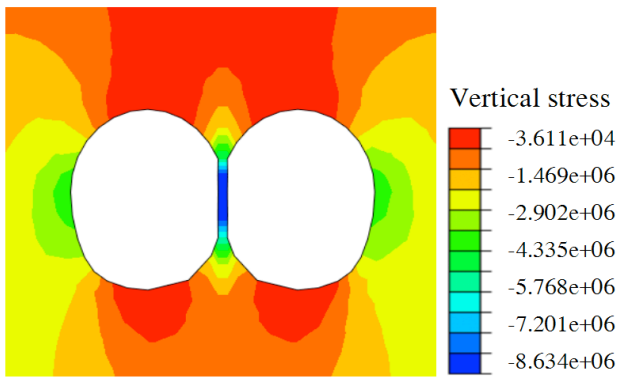


(b) Q-type cross-section

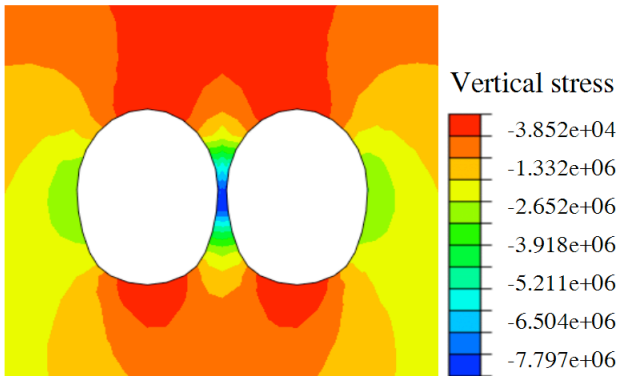


(c) R-type cross-section

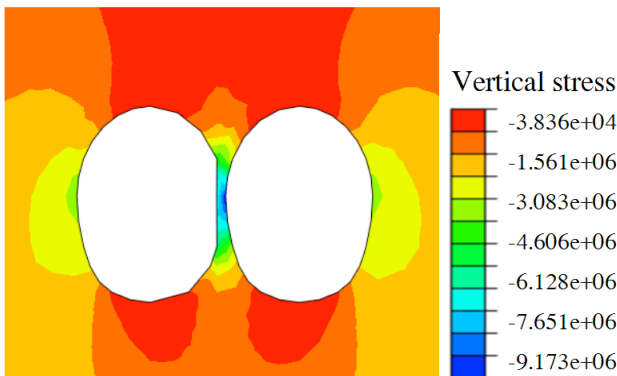
Fig. 5. Plastic failure zones in the grade V surrounding rocks of three cross-sections tunnels



(a) P-type cross-section



(b) Q-type cross-section



(c) R-type cross-section

Fig. 6. Vertical stress distribution in the grade V surrounding rocks of three cross-section tunnels

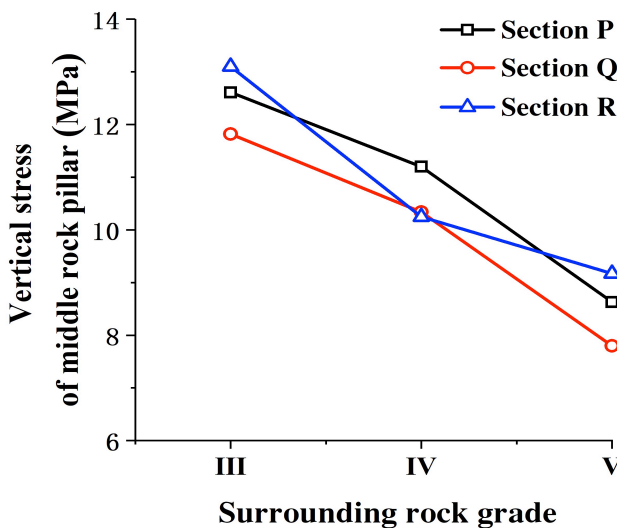


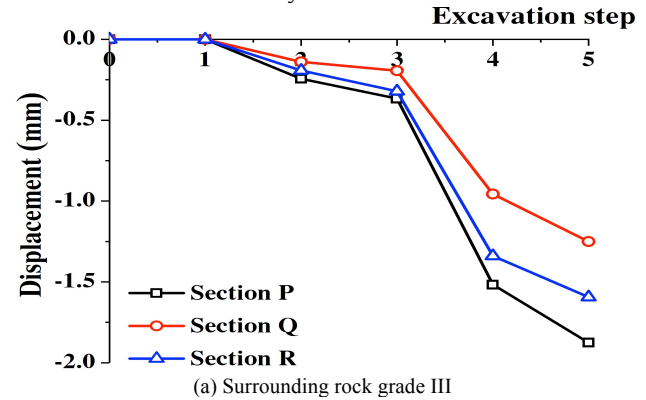
Fig. 7. Vertical stress in the rock pillar of three cross-section tunnels for different surrounding rock grades

As seen from Figure 7, it can be found that the grade change of the surrounding rock is very sensitive to the maximum vertical stress in the rock pillar of the tunnels, and the higher grade of the surrounding rock, the smaller vertical stress at the waist of the middle rock pillar.

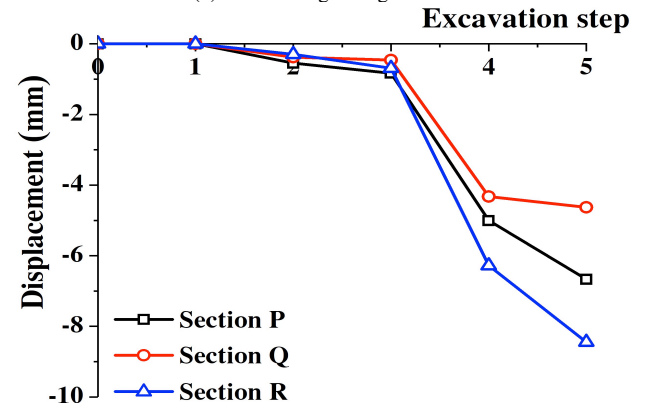
4.3 Vertical displacement of the middle rock pillar

As seen from Figure 8, the vertical displacements of the monitoring point 1 increase with the excavation steps increasing for different surrounding rock grades. For the maximum vertical displacements in three cross-section tunnels with surrounding rock grades □, Q-type cross-section is the smallest, P-type cross-section is the biggest, and R-type cross-section is in the middle.

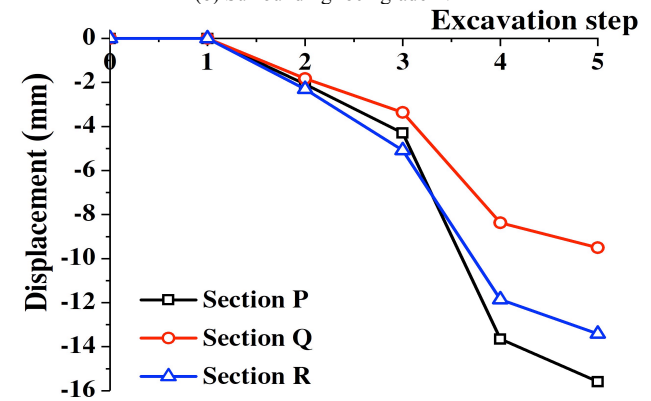
It can be seen from Figure 9 that the grade change of the surrounding rock is very sensitive to the maximum vertical displacement in the rock pillar of the tunnels, and the higher grade of the surrounding rock, the higher vertical displacement at the monitoring point 1 of the middle rock pillar. Especially the surrounding rock grade is more than □, the maximum vertical displacement of the monitoring point 1 has increased dramatically.



(a) Surrounding rock grade III



(b) Surrounding rock grade IV



(c) Surrounding rock grade V

Fig. 8. Vertical displacement of the monitoring point 1 for three cross-section tunnels with different surrounding rock grades

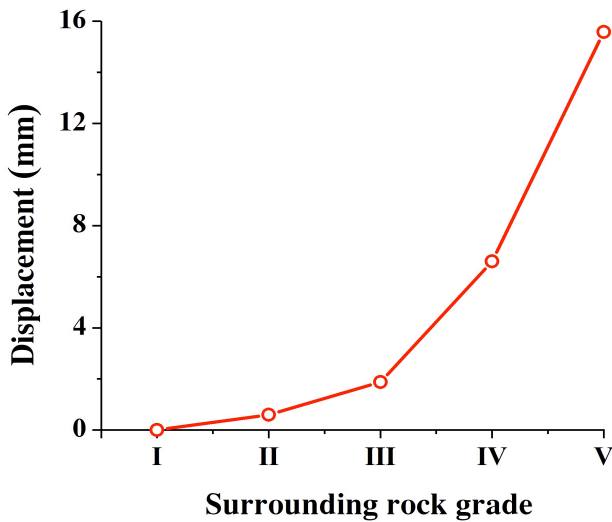


Fig. 9. Vertical displacements of the monitoring point 1 of the P-type cross-section tunnel with different surrounding rock grades

4.4 Horizontal displacement skew effect analysis

The horizontal displacements of monitoring points 2 and 3 for three cross-section tunnels with surrounding rocks grade V are shown in Figure 10.

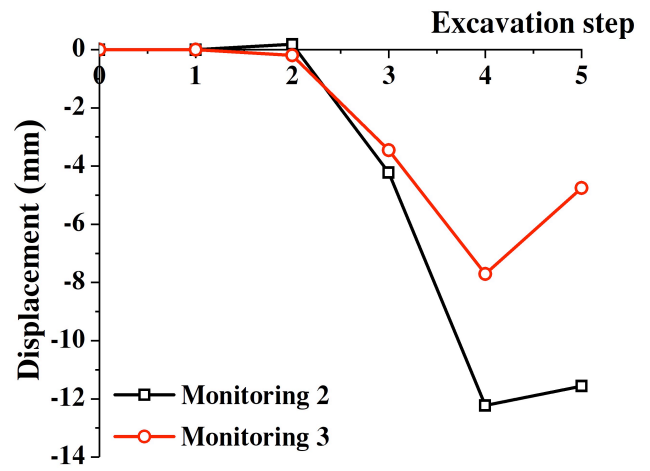
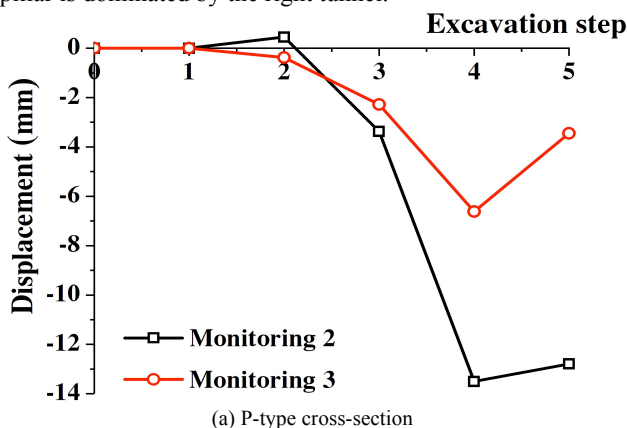
It can be found that the horizontal displacements of these monitoring points shift to the left tunnel, regardless of the cross-section types. In addition, at the initial excavation steps from 1 to 3, the horizontal displacements of the monitoring points show a small difference in magnitude, while in the excavation steps 4 and 5, the horizontal displacement differences between left and right tunnels gradually increases. This shows that the skew displacement effect on both sides of the middle rock pillar gradually increases with the excavation steps increasing.

To quantitatively analyse the horizontal displacement skew effect of the rock pillar during the excavation of ultra-small spacing subway tunnels, the skew coefficient K is defined as follows:

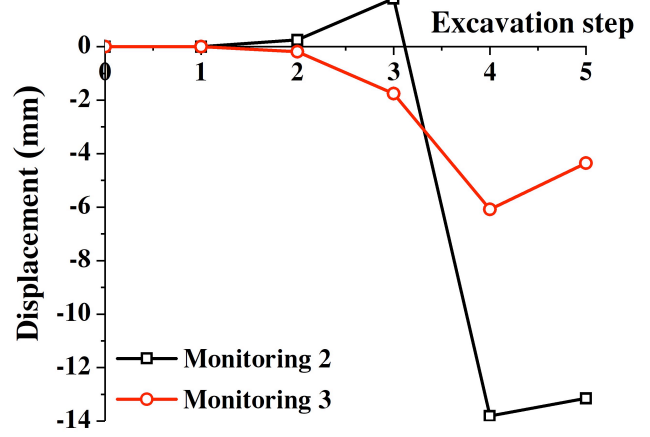
$$K = \left| \frac{D_1}{D_2} \right| \tag{6}$$

where D_1 is the horizontal displacement monitoring point 2 of left tunnel, and D_2 is the horizontal displacement monitoring point 3 of right tunnel.

In Equation (6), when $K > 1$, the horizontal displacement of the rock pillar is dominated by the left tunnel. When $K = 1$, the horizontal displacement of the rock pillar is symmetrical. When $K < 1$, the horizontal displacement of the pillar is dominated by the right tunnel.



(b) Q-type cross-section



(c) R-type cross-section

Fig. 10. Horizontal displacements of the monitoring points for different cross-section tunnels with surrounding rock grade V

As shown in Figure 11, the horizontal displacement skew coefficient K for three cross-section tunnels increases with the excavation steps increasing. It can be found that the skew effect of the middle rock pillar during the ultra-small spacing tunnel excavation is significant, and the horizontal displacement of the pillar is mainly inclined towards the left tunnel. For the skew coefficient K in three cross-section tunnels, Q-type cross-section is the smallest, P-type cross-section is the biggest, and R-type cross-section is in the middle.

4.5 Vertical stress calculation verification analysis

Taking the P-type cross-section tunnel with surrounding rock grade V as an example, the ultimate load on the middle rock pillar can be obtained by using Equation (5). $L=4.0$ m, a and H are known in the practical engineering.

In addition, it can be seen from Figure 5(a) that the plastic zones of the middle rock pillar penetrate completely under these conditions, and the value of Y is therefore half a . On the other hand, the actual bearing load of the middle rock pillar can be calculated by using Equation (3). Substituting the related data, it can be obtained $\sigma_p=8.67$ MPa, $\sigma_s=0.40$ MPa. $\sigma_p \gg \sigma_s$ meaning that the ultimate load on the middle rock pillar is far less than the actual load value. This result is consistent with the results of numerical simulation.

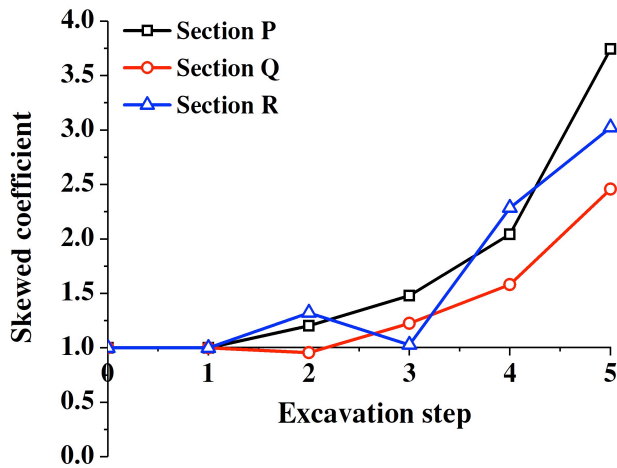


Fig. 11. Variation in the skew coefficient of the middle rock pillar for the three cross-section tunnels with surrounding rock grade V

In summary, the middle rock pillar in a P-type cross-section tunnel with surrounding rock grade V is in a unstable state, and the effective reinforcement measures must be taken to ensure the stability of the rock pillar and the construction safety of the ultra-small spacing tunnels.

5. Conclusions

In order to study the stability of the middle rock pillar in the ultra-small spacing subway tunnels, the plastic zone of the surrounding rock, the stress distribution and skew displacement effect of the middle rock pillar were analyzed with theoretical and numerical comparing methods, the conclusions are as follows:

(1) For plastic zones of the surrounding rock, the maximum vertical displacement, and the maximum vertical stress in the rock pillar, Q-type section tunnels is always the best option.

(2) The skew effect of the middle rock pillar during the ultra-small spacing tunnel excavation is significant, and the horizontal displacement of the pillar is mainly inclined towards the left tunnel. For the skew coefficient K in three cross-section tunnels, Q-type cross-section is the smallest one.

(3) For evaluating the stability of the middle rock pillar of ultra-small spacing, a theoretical method is derived and it is verified effectively.

The above investigations only considered in two-dimension. However, the practical engineering is actually a three-dimension problem, so the 3D researches should be studied in the future.

Acknowledgements

This work was financially supported by the National Natural Science Foundation of China (51774112; 51474188), the International Cooperation Project of Henan Science and Technology Department (182102410060), the Doctoral Fund of Henan Polytechnic University (B2015-67), and Taihang Scholars Program. All these are gratefully appreciated.

This is an Open Access article distributed under the terms of the Creative Commons Attribution License



References

- Chehade, F. H., Shahrour, I., "Numerical analysis of the interaction between twin-tunnels: Influence of the relative position and construction procedure". *Tunnelling & Underground Space Technology*, 23(2), 2008, pp. 210-214.
- Siahmansouri, A., Gholamnejad, J., Marji, M. F., "A hybridized numerical and regression method for estimating the minimum rock pillar width of twin circular tunnels". *Arabian Journal of Geosciences*, 7(3), 2014, pp. 1059-1066.
- Lim, H., Son, K., "The stability analysis of near parallel tunnels pillar at multi-layered soil with shallow depth by numerical analysis". *Korean Society of Geoenvironment Society Symposium*, 15(1), 2014, pp. 369-377.
- Mortazavi, A., Hassani, F. P., Shabani, M., "A numerical investigation of rock pillar failure mechanism in underground openings". *Computers & Geotechnics*, 36(5), 2009, pp. 691-697.
- Chen, S. L., Lee, S. C., Gui, M. W., "Effects of rock pillar width on the excavation behavior of parallel tunnels". *Tunnelling & Underground Space Technology Incorporating Trenchless Technology Research*, 24(2), 2009, pp. 148-154.
- Zhang, W., Goh, A. T. C., "Numerical study of pillar stresses and interaction effects for twin rock caverns". *International Journal for Numerical & Analytical Methods in Geotechnics*, 39(2), 2015, pp. 193-206.
- Yang, J. H., Wang, S. R., Li, C. L., Li, Y., "Disturbance Deformation Effect on the Existing Tunnel of Asymmetric Tunnels with Small Spacing". *Disaster Advances*, 6(13), 2013, pp. 269-277.
- Wang, S. R., Li, C. L., Li, D. J., Zhang, Y. B., Hagan, P., "Skewed pressure characteristics induced by step-by-step excavation of double-arch tunnel based on infrared thermography". *Tehnicky Vjesnik-Technical Gazette*, 23(3), 2016, pp. 827-833.
- Wang, G., Liao, J., Zhang, Y., Wang, G., "Study on safe clear distance and mechanical characteristics of middle rock pillar for shallow large-span tunnel with small clear distance". *Geotechnical Investigation & Surveying*, 39(4), 2011, pp. 18-23.
- Wang, S. R., Li, C. L., Wang, Y. G., Zou Z. S., "Evolution characteristics analysis of pressure-arch in double-arch tunnel". *Tehnicky Vjesnik-Technical Gazette*, 23(1), 2016, pp. 181-189.
- Yan, L., "Stability analysis of middle rock pillar in parallel tunnels in horizontal inter-bedding rock mass". *Chinese Journal of Rock Mechanics and Engineering*, 28(S₁), 2009, pp. 2898-2904.
- Wang, H., Chen, W. Z., Chen, P. S., Tian, H. M., Zhao, W. S., "Study of section morphology and reasonable distance optimization of large-span twin tunnels with small clear spacing in shallow rock mass". *Rock and Soil Mechanics*, 2011, 32(S₂), 2011, pp. 641-646.
- Gu, H. Y., "Section optimization and design parameters study on large-spanned small-spaced twin-tube tunnel". *Railway Standard Design*, 2013(2), 2013, pp. 85-89.
- Han, X. M., Sun, M., Li, W. J., Zhu, Y. Q., "Optimization of section shape and support parameters of tunnel under complicated conditions". *Rock and Soil Mechanics*, 32(S₁), 2011, pp. 725-731.
- He, Z. K., "Research on reasonable spacing of double-hole tunnel based on stress analysis of middle rock pillar". *Highway*, 59(5), 2014, pp. 26-29.
- Wang, X. C., Huang, F. C., Zhang, H. X., Zhang, L. G., "Discussion and improvement for A. H. Wilson's coal pillar design". *Journal of China Coal Society*, 27(6), 2002, pp. 604-608.